PCCP

Accepted Manuscript

ROYAL SOCIETY OF CHEMISTRY

www.rsc.org/pccp

Journal Name

COMMUNICATION

The effect of sulfur on the electrical property of S-N co-doped ZnO thin film: experiment and first-principles calculation

Received 00th January 20xx,
Accepted 00th January 20xx

DOI: 10.1039/x0xx00000x

www.rsc.org/

Wenzhe Niu, Hongbin Xu, Yanmin Guo, Yaguang Li, Zhizhen Ye and Liping Zhu*

P-type sulphur-Nitrogen (S-N) co-doped ZnO thin films were deposited. The effect of sulphur on the electrical properties were discussed. First-principles calculations indicate it is most stable when the S atom is close to the N atom in the (0002) plane, implying that the dual-doped ZnO is relative feasible to approach. The partial density of states of S-N co-doped ZnO showed that the S impurity played a vital role in forming the p-type conductivity.

ZnO, as a promising semiconductor material to achieve commercial blue and ultraviolet light emitting devices (LEDs) and laser diodes (LDs),[1] has attracted increasing attention, due to its direct wide band gap of 3.37 eV and large exciton binding energy (60 meV) at room temperature.[2,3] However, preparing p-type ZnO with high quality and stable electrical property for fabricating ZnO homojunctions is still a challenge up to now.[3] Compensation of native donor defect, low solubility of acceptor dopant and high activation energy are the major hurdle to achieve p-type ZnO.[4] N, possessing one electron less than O, is regarded as possible accepter when doped into ZnO, which have been tried before. But the results obtained, both in experiment[5, 6] and in calculation[7, 8], by different groups are controversial.[5-7,9] There are also attempts to get p-type conductivity by co-doping. Lu *et al* realized p-type ZnO with lowest resistivity of 57.3 Ωcm, Hall mobility of 0.43 $cm^2V^{-1}s^{-1}$ and carrier concentration of 2.25×10^{17} cm^{-3} by Al-N co-doping.[10] S is usually used for the realization of band gap engineering of ZnO and $ZnO_{1-x}S_x$ thin films have been achieved by different methods, such as pulsed laser deposition (PLD),[11] atomic layer deposition (ALD)[12] and radio frequency magnetron sputtering.[13,14] Xu *et al* investigated the composition dependence of the band gap energy in $ZnO_{1-x}S_x$ system.[14] Persson *et al* researched the $ZnO_{1-x}S_x$ alloy by calculation and experimental, drawing a conclusion that the valence band bowing of $ZnO_{1-x}S_x$ alloy in its O-rich side can enhance N doping with lower formation energy. And N_O possesses shallower accepter state in the band gap, attributing to the rise of valence band maximum.[15] However, to the best of my knowledge, few works about S-N co-doped ZnO film were published.

In this paper, we investigated the deposition condition of S-N co-doped ZnO film grown by radio frequency magnetron sputtering and their crystal structure and electrical properties. Moreover，first calculation study was performed to confirm the effect of S atom in the dual-doped ZnO.

All the samples in the experiment were grown on the glass substrates by RF magnetron sputtering technique (PVD-75, Kurt J. L. Lesker). A ZnO and a ZnS ceramic target with high purity of 99.99% were used for depositing N-mono doped ZnO and S-N co-doped ZnO respectively. Argon (Ar) and N_2O were served as working gas and reactive gases respectively. Before loaded into the growth chamber, the substrates were cleaned in an ultrasonic bath using acetone, ethanol and de-ionized

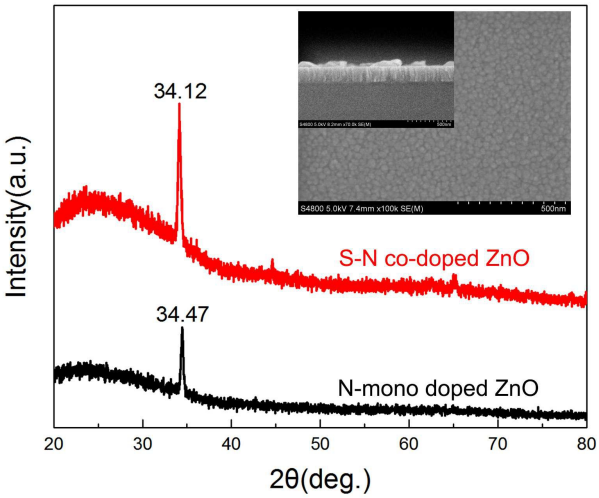

Fig.1 XRD pattern of annealed sample N2 and SN4. (Insert) Top view and cross section SEM images of S-N co-doped ZnO film with the N_2O: Ar=1:1 at 450^{0}C.

[a] Address here.
[b] Address here.
[c] Address here.

† Footnotes relating to the title and/or authors should appear here. Electronic Supplementary Information (ESI) available: [details of any supplementary information available should be included here]. See DOI: 10.1039/x0xx00000x

water for 15 minutes each, successively, and then dried by nitrogen gas blow. The vacuum chamber was evacuated to a base pressure of 5×10^{-6} Torr and the substrate was heated to growing temperature. A total 3mTorr gas, including the working gas and reactive gas, were introduced into the chamber. For N-mono doped ZnO, samples with N_2O/Ar of 20% and 100% were grown, which were named N1 and N2. In the contrast experiment, different N_2O partial pressures were adopted for S-N co-doped ZnO to find the optimal parameter. Sample SN1-SN4 present the thin films deposited under the N_2O/Ar of 20%, 50%, 75% and 100% respectively. These samples were deposited at 450^{O}C. All samples ware annealed at 600^{O}C with N_2 as the protective gas for 1 hour and cooled down at room temperature.

X-ray diffraction (XRD) with a Cu Kα1 (λ=1.5406Å) source was used to characterize the crystal structure. The surface morphology and thickness of the films were observed by scanning electron microscopy (SEM). The electrical properties were measured by Hall measurements in the van der Pauw configuration at room temperature. The chemical state was investigated with X-ray photoelectron spectroscopy (XPS).

To confirm the formation of ZnO-based film, XRD measurement was used to characterize the crystal structure. Fig.1 shows XRD patterns of N-mono ZnO and S-N co-doped ZnO films grown under the atmosphere that N_2O/Ar is 100%. As shown in the Figure, a single diffraction peak is observed in each curve, which is corresponding to ZnO (0002) plane. A clear shift of (0002) peak to the lower diffraction value can be observed, which is also found in S-doped ZnO alloy due to the larger atomic radius than O.[14] Moreover, the intensity of (0002) peak of sample SN4 is stronger than that of sample SN1 (see Fig. S1), indicating that higher N_2O partial pressure with abundant O atoms contributes to the better ZnO crystal quality. Insert figure in Fig. 1 depicts the SEM morphology of S-N co-doped ZnO film deposited under the N_2O/Ar ratio of 1:1 at 450^{O}C. The film is composed of uniform grains and columnar-grained structure perpendicular to the substrate can be clearly distinguished from the cross section image, showing the structure of the doped film do not change which also will be verified from the XRD pattern.

The resistivity and Hall measurements of the annealed doped ZnO films were performed and the experimental data is listed in Table 1. The measurement results show the two N-mono doped samples (N1 and N2) are n-type conductivity. As the counterparts, S-N co-doped ZnO thin films were deposited using a ZnS target under the same condition. These samples,

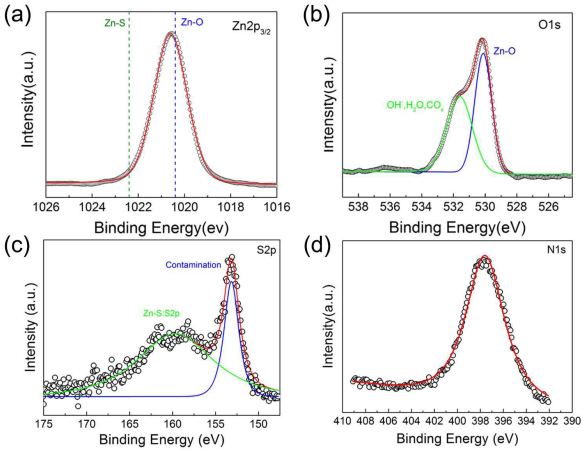

Fig.2 Narrow-scan XPS spectra of (a) Zn 2p3/2, (b) O 1s, (c) S 2p and (d)N 1s in S-N co-doped ZnO thin film (sample SN4).

no matter how many the N_2O/Ar ratio is, all show p-type conductivity, indicating S might play a crucial role in changing the electrical property of ZnO thin film.

XPS analysis was performed to investigate the chemical states of S and N in the co-doped ZnO thin film (sample SN4). All signals of the spectra have been calibrated by the standard C1s photoelectron signal at 284.8 eV. The XPS spectra in the range of 0-600 eV shows the signals from Zn, O, S, and N are detected, demonstrating S-N co-doped ZnO thin film was deposited successfully. Fig. 2(a)-(d) gives the narrow-scan XPS spectra of Zn 2p3/2, O 1s, S 2p and N 1s respectively. The binding energy of Zn 2p3/2 is located at 1020.59 eV which is close to the value of ZnO (1020.4 eV) and below to that of ZnS (1022.4 eV),[16] suggesting the chemical states of Zn is an intermediate states between ZnS and ZnO but is more close to the ZnO side. This is attributed to the formation of Zn-S bond in the film while the ZnO is still the host material.[14] The O1s signals have two peak which can be fitted by the Lorentzian distribution. The signals from O sited in the ZnO lattice is corresponding to the lower energy peak at 530.14 eV while the higher energy peak at 531.61 eV is usually attributed to the surface contamination(*e.g.* carbon oxides, water, hydroxide and *et al.*). The incorporation of both S and N is clearly demonstrated by the spectra of S 2p and N1s. The peak at 160.39 eV of S2p originates from S with -2 valence. However, a strong peak at 152.6 eV is detected beside the signal of S^{2-}. By consulting the existing database and literature, the signal does not match with S, SO_2, SO_3^{2-} or any other sulfur containing

TABLE 1 Electrical properties of S-N co-doped ZnO grown under different N_2O/Ar and the contrastive N doped ZnO thin film.

Sample	N_2O/Ar(%)	Resistivity(Ωcm)	Hall mobility ($cm^2V^{-1}s^{-1}$)	Carrier concentration(cm^{-3})	type
N1	20	0.7357	0.996	8.52×10^{18}	n
N2	100	0.5076	2.99	4.11×10^{18}	n
SN1	20	125.7	1.4	3.54×10^{16}	p
SN2	50	611.2	1.47	6.97×10^{15}	p
SN3	75	237.6	0.97	8.96×10^{15}	p
SN4	100	21.46	0.649	4.48×10^{17}	p

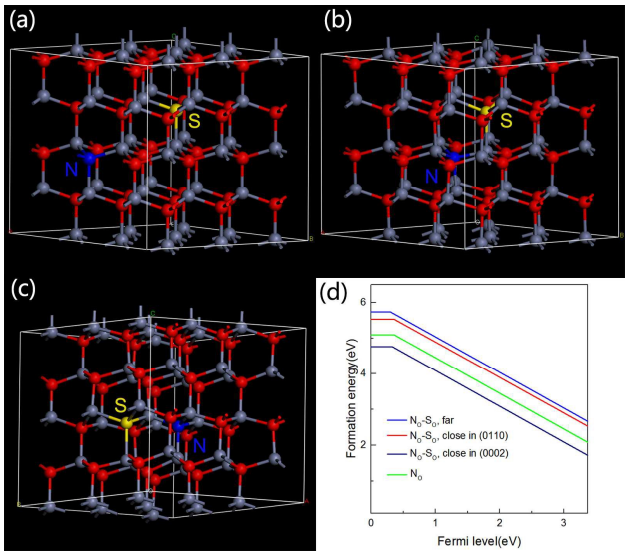

Fig.3 The positioning illustration of calculated S and N atoms in oxygen sites: (a) S atoms are away from the N, (b) S and N atoms are connected to the same Zn atom in (0110) plane, (c) S and N atoms are connected to the same Zn atom in (0002) plane. (d) Formation energies of doped S and N in ZnO as a function of the Fermi level, obtained from GGA calculations and referenced to the energy of a free O_2 molecule.

compounds. Thereby, we believe that the peak originate from other contamination. As can we see, from the intensity of peaks, only a small fraction of S are doped into the film in the form of Zn-S bond. Even so, no other phases (*e.g.* $ZnSO_4$) are observed in the XRD pattern and the semiconductor converts to p-type with the S doped, contrasting to the N-doped ZnO. This is associated with the raise of valence band maximum caused by the formed Zn-S bonds, making the N_O to be shallower acceptor. The peak of N1s is found at 398.09 eV, which is regarded as the signals from O-Zn-N in the literature.

The effect of temperature on the chemical state of S was researched. We fixed the growing atmosphere at N_2O/Ar=100% and deposited the co-doped ZnO films at 300 ^{O}C, 400 ^{O}C, 450 ^{O}C and 500 ^{O}C. These samples are named E1 to E4 respectively. Fig. S2 summarizes the electrical properties of sample E1-E4. The carrier concentration and mobility increase while the resistivity decreases with the temperature go up until 450 ^{O}C, where the thin film possess best electrical property. This is mainly attributed to the enhancement of the crystal quality, which is evidenced by XRD pattern shown in Fig. S3. However, sample E4 shows a worse performance than sample E3. From the XPS measurements depicted in Fig. S4(a), we find two strong peaks at 168.98 eV and 170.14 eV are corresponding to S2p3/2 and S2p1/2 of S with +6 valence respectively while the peak at 160.39 eV of S2p originates from S with -2 valence is much weak. It means that higher temperature improve the oxidation of S, resulting a worse electrical conductivity. Fig. S4(b) indicates the peak of N almost remains unchanged when the temperature increase, making clear the dominant factor that effecting the electrical property is the doped S atom and its chemical states.

To further study the origin of p-type conductive property, we have calculated the formation energy and density of states of S-N co-doped ZnO with S-N at different relative positions. All

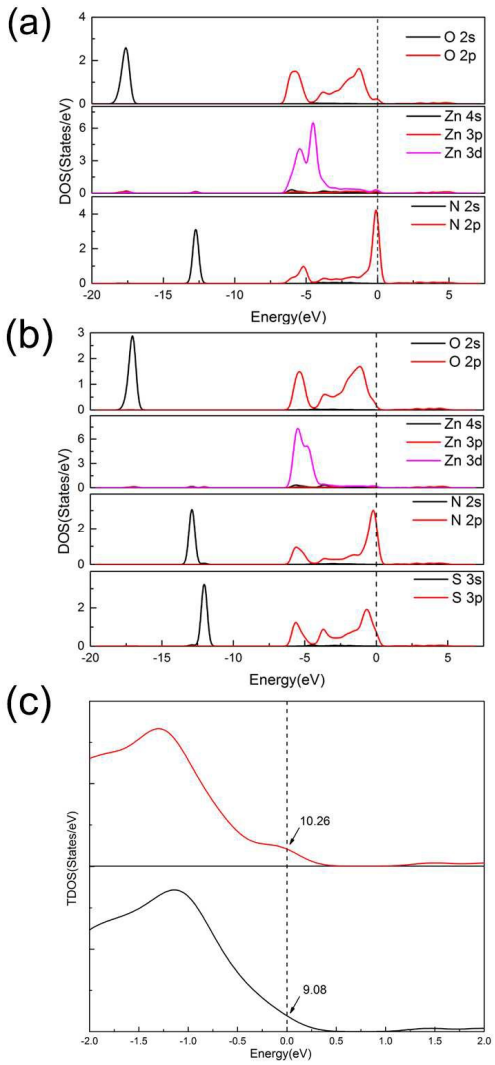

Fig.4 PDOS of (a) N-doped ZnO and (b) S-N co-doped ZnO, where the S atom is close to the N atom in the (0002) plane. (c) Amplified TDOS of N-doped ZnO and S-N co-doped ZnO.

the calculations are carried out using the DFT based on the commercial version of the software package CASTEP (Cambridge Sequential Total Energy Package), which could offer vibrational properties of adsorption and accurate calculations of energy. The ZnO structure in application is a wurtzite structure. Structural parameters for ZnO films are: a = 3.249 Å and c/a = 1.603. A 3×3×2 supercell (36 zinc atoms and 36 oxygen atoms) was built and two O atoms were substituted by one S atom and one N atom. As we know, the atomic radius of both nitrogen and sulphur are bigger than oxygen atom. It is preferred that the doped S and N impurity occupy the oxygen site. Three kinds of relative positions of S and N are considered: sulphur impurities are placed at oxygen sites away from nitrogen, sulphur and nitrogen atoms are connected to the same zinc atom in (0110) plane or in (0002) plane. The relative positions are illustrated in Fig. 3(a)-(c).The formation energy of a supercell with the defects is an important physical quantity to determine the solubility of the dopants.[17] The

formation energy of S-N co-doped ZnO in charge state q is defined as: [18]

$$E^{f}\left(\mathrm{N_O^q}\text{-}\mathrm{S_O}\right) = E^{tot}\left(\mathrm{N_O^q}\text{-}\mathrm{S_O}\right) - E^{tot}\left(\mathrm{ZnO,bulk}\right) + 2\mu_{\mathrm{O}} - \mu_{\mathrm{S}} - \mu_{\mathrm{N}} + \mathrm{q}\left(E_{\mathrm{F}} + E_{VBM}\right) \quad , \qquad (1)$$

where $E^{tot}\left(\mathrm{N_O^q}\text{-}\mathrm{S_O}\right)$ is the total energy from a supercell calculated with one S impurity and one N impurity, both of which occupy the oxygen site, and $E^{tot}(\mathrm{ZnO,\ bulk})$ is the total energy for the equivalent supercell containing only bulk ZnO. E_F is the Fermi level, referenced to the valence band maximum (VBM) in the bulk. E_{VBM} is the energy of the bulk ZnO VBM. The chemical potentials μ_O, μ_S, μ_N represent the energies of replaced O atom, incorporated S impurity and N impurity respectively. Here, the N_2O is abundant in the chamber, so we believe that it is O-rich condition. Thus, the value of μ_O is fixed to half of the energy of an O_2 molecule. Then, $\mu_{Zn} = \mu_{ZnO} - \mu_{O_2}/2$, $\mu_N = \left(\mu_{N_2O} - \mu_{O_2}/2\right)/2$, $\mu_S = \mu_{ZnS} - \mu_{Zn}$. The calculated chemical potentials of O, S and N are -433.81eV, -286.07eV and -265.85eV respectively.

The calculated formation energies are plotted as a function of E_F are shown in Fig. 3(d). The high defects formation energy indicates a low solubility of dopants and results in low concentrations of charge carriers. Under O-rich conditions, it is most stable when the N_O is close to the S_O in the (0002) plane. What's more, the formation energy is lower than N-mono doped ZnO by 0.33 eV, which means the S-N dual-doped ZnO is more stable than the N-mono doped ZnO. In the energy-lowest module, the volume of the co-doped ZnO structure increase compared to the pure ZnO. It attributed that the longer Zn-S bond is formed in the co-doped structure. In addition, the Zn-O bond is also slightly increased, which is corresponding to the shift of diffraction angle in XRD measurement. More details about the optimized bond lengths and lattice parameters are listed in Table S1.

The partial DOS (PDOS) of the N-doped ZnO and S-N co-doped ZnO, illustrated in Figs. 4(a) and 4(b), are calculated to examine the electronic structures in which the zero energy corresponds to the Fermi level. The localized state near the Fermi level comes mainly from the N 2p states, which is also attributed to the O 2p states around the Fermi level. The DOS of S-N co-doped ZnO has some changes compared with Fig. 4(a). The DOS of O 2p and Zn 3d around the Fermi level are weaken while the N 2p states show a strong coupling effects with the S 3p state. Compared to N 2s state in N-mono doped ZnO, the Fermi level shifts upward slightly, thereby making the N atom acting as a shallower acceptor. The calculated amplified total DOS near the Fermi-level of N-mono and S-N co-doped ZnO are shown in Fig. 4(c). Even though the integrated areas from the Fermi-level to the VBMs illustrated that the N-mono doped ZnO possess slightly more holes carrier than S-N co-doped structure,[19] p-type conductivity dependent not only on the number of holes carrier, but also other carrier motilities, *e.g.* the effective hole masses and carrier mobilities.[20] Here, the calculation results shows that the S impurity decease the formation energy of dual-doped ZnO and make the N_O to be a shallower accepter, which is believed to form an easier p-type conductive ZnO.

Conclusions

In summary, S-N co-doped ZnO thin films with p-type conductivity were deposited using N_2O as the source of O and N. By optimizing N_2O/Ar flow ratio, the co-doped ZnO thin films with well p-type electrical properties was fabricated. The effects of growing temperature on the electrical property are investigated. XPS spectra shows both S and N exist in the films. P-type conductive ZnO thin film with the resistivity, mobility and hole concentration of 21.46 Ωcm, 0.649 $cm^2V^{-1}s^{-1}$ and 4.482×10^{17} cm^{-3} respectively was obtained. S-N co-doped ZnO is more stable than N-mono doped ZnO when the S atom is close to the N atom in (0002) plane, calculated by first-principles study. Moreover, the S 3p state makes the N atom to be a shallower acceptor.

This work was supported by National Natural Science Foundation of China 51372224 and 91333203, Program for Innovative Research Team in University of Ministry of Education of China (IRT13037).

Notes and references

1 Y. I. Alivov, E. V. Kalinina, A. E. Cherenkov, D. C. Look, B. M. Ataev, A. K. Omaev, M. V. Chukichev, and D. M. Bagnall, *Appl. Phys. Lett.*, 2003, **83**, 4719-4721.
2 T. Gruber, C. Kirchner, R. Kling, F. Reuss, A. Waag, F. Bertram, D. Forster, J. Christen, and M. Schreck, *Appl. Phys. Lett.*, 2003, **83**, 3290-3292.
3 D. C. Look, *Mater. Sci. Eng. B*, 2001, **80**, 383-387.
4 S. Dhara and P. K. Giri, *Thin Solid Films*, 2012, **520**, 5000-5006.
5 D. C. Look, D. C. Reynolds, C. W. Litton, R. L. Jones, D. B. Eason, and G. Cantwell, *Appl. Phys. Lett.*, 2002, **81**, 1830-1832.
6 A. V. Singh, R. M. Mehra, A. Wakahara, and A. Yoshida, *J. Appl. Phys.*, 2003, **93**, 396-399.
7 E. C. Lee, Y. S. Kim, Y. G. Jin, and K. J. Chang, *Phys. Rev. B*, 2001, **64**, 085120.
8 J. L. Lyons, A. Janotti, and C. G. Van de Walle, *Appl. Phys. Lett.*, 2009, **95**, 252105.
9 T. M. Barnes, K. Olson, and C. A. Wolden, *Appl. Phys. Lett.*, 2005, **86**, 112112.
10 J. G. Lu, Z. Z. Ye, F. Zhuge, Y. J. Zeng, B. H. Zhao, and L. P. Zhu, *Appl. Phys. Lett.*, 2004, **85**, 3134-3135.
11 Y. Z. Yoo, Z. W. Jin, T. Chikyow, T. Fukumura, M. Kawasaki, and H. Koinuma, *Appl. Phys. Lett.*, 2002, **81**, 3798-3800.
12 C. Platzer-Björkman, T. Törndahl, D. Abou-Ras, J. Malmström, J. Kessler, and L. Stolt, *J. Appl. Phys.*, 2006, **100**, 044506.
13 B. K. Meyer, A. Polity, B. Farangis, Y. He, D. Hasselkamp, Th. Krämer, and C. Wang, *Appl. Phys. Lett.*, 2004, **85**, 4929-4931.
14 H. B. Xu, L. P. Zhu, J. Jiang, H. Cai, W. F. Chen, L. Hu, Y. M. Guo, and Z. Z. Ye, *J. Appl. Phys.*, 2013, **114**, 083522.
15 C. Persson, C. Platzer-Bjorkman, J. Malmstrom, T. Torndahl, and M. Edoff, *Phys. Rev. Lett.*, 2006, **97**, 146403.
16 Y. He, L. Wang, L. Zhang, M. Li, X. Shang, Y. Fang, and C. Chen, *J. Alloys Compd.*, 2012, **534**, 81-85.
17 P. Erhart, A. Klein, and K. Albe, *Phys. Rev. B*, 2005, **72**, 085213.

18 W. Chen, L. Zhu, Y. Li, L. Hu, Y. Guo, H. Xu, and Z. Ye, *Phys. Chem. Chem. Phys.*, 2013, **15**, 17763-17766.
19 H. Li, Y. Lv, J. Li, and K. Yu, *Phys. Scr.*, 2015, **90**, 025803.
20 H. Li, Y. Lv, H. Fu, J. Li, and K. Yu, *J. Appl. Phys.*, 2015, **117**, 055701.